Table VI. Principal Combination Band Progressions Observed in the Resonance Raman Spectra of $Rh_2(O_2CCH_3)_4L_2$ (L = PPh_3, $AsPh_3$, $SbPh_3$)

ν_1 band progressions		ν_2 band progressions	
from	to	from	to
	PPh_3 Complex[8]		
$\upsilon_1\nu_1$	$\upsilon_1 = 4$	$\upsilon_2\nu_2$	$\upsilon_2 = 2$
$\upsilon_1\nu_1 + \nu_2$	$\upsilon_1 = 3$		
$\upsilon_1\nu_1 + 2\nu_2$	$\upsilon_1 = 2$		
$\upsilon_1\nu_1$ + q X-sens	$\upsilon_1 = 2$		
$\upsilon_1\nu_1$ + 305	$\upsilon_1 = 2$		
	$AsPh_3$ Complex		
$\upsilon_1\nu_1$	$\upsilon_1 = 7$	$\upsilon_2\nu_2$	$\upsilon_2 = 3$
$\upsilon_1\nu_1 + \nu_2$	$\upsilon_1 = 7$	$\upsilon_2\nu_2 + \nu_1$	$\upsilon_2 = 2$
$\upsilon_1\nu_1 + \delta$(OCO)	$\upsilon_1 = 6$	$\upsilon_2\nu_2 + \delta$(OCO)	$\upsilon_2 = 2$
$\upsilon_1\nu_1 + 2\nu_2$	$\upsilon_1 = 6$		
$\upsilon_1\nu_1 + \nu_2 + \delta$(OCO)	$\upsilon_1 = 4$		
$\upsilon_1\nu_1 + 2\nu_2 + \delta$(OCO)	$\upsilon_1 = 3$		
$\upsilon_1\nu_1$ + p-ring	$\upsilon_1 = 2$		
$\upsilon_1\nu_1$ + r X-sens	$\upsilon_1 = 2$		
$\upsilon_1\nu_1$ + t X-sens	$\upsilon_1 = 2$		
$\upsilon_1\nu_1$ + 321	$\upsilon_1 = 2$		
	$SbPh_3$ Complex		
$\upsilon_1\nu_1$	$\upsilon_1 = 6$	$\upsilon_2\nu_2$	$\upsilon_2 = 4$
$\upsilon_1\nu_1 + \nu_2$	$\upsilon_1 = 5$	$\upsilon_2\nu_2 + \nu_1$	$\upsilon_2 = 4$
$\upsilon_1\nu_1$ + t X-sens	$\upsilon_1 = 5$	$\upsilon_2\nu_2 + \delta$(OCO)	$\upsilon_2 = 2$
$\upsilon_1\nu_1 + 2\nu_2$	$\upsilon_1 = 4$		
$\upsilon_1\nu_1 + 3\nu_2$	$\upsilon_1 = 3$		
$\upsilon_1\nu_1 + \delta$(OCO)	$\upsilon_1 = 3$		
$\upsilon_1\nu_1$ + r X-sens	$\upsilon_1 = 2$		
$\upsilon_1\nu_1 + \nu_2 + \delta$(OCO)	$\upsilon_1 = 2$		

∠CMC in the coordinated ligand, which decreases in the order 103.2, 101.5, and 99.7° for M = P,[13] As,[2] and Sb,[2] respectively. The principal X-sensitive (X-sens) modes involved in this coupling are the p, q, r, t, and y modes. The δ(OCO) mode is, interestingly, also involved in combination band progressions with both ν_1 and ν_2, indicating that slight structural changes on $\sigma \rightarrow \sigma^*$ excitation must occur throughout the acetate rings.

Excitation profiles have been constructed for the ν_1, ν_2, $2\nu_1$, $\nu_1 + \nu_2$, $2\nu_2$, and δ(OCO) bands of $Rh_2(O_2CCH_3)_4(AsPh_3)_2$ and for the ν_1, ν_2, t X-sens, ν_1 + t X-sens, $2\nu_1$, $\nu_1 + \nu_2$, r X-sens, $2\nu_2$, and δ(OCO) bands of $Rh_2(O_2CCH_3)_4(SbPh_3)_2$ (Figures 6 and 7). As is the case for the excitation profiles of the analogous triphenylphosphine complex,[8] all the Raman bands maximize under the contour of the resonant electronic band. Depolarization ratios were obtained on resonance for the ν_1 band of $Rh_2(O_2CCH_3)_4(AsPh_3)_2$ and for the ν_1, ν_2, and t X-sens bands of $Rh_2(O_2CCH_3)_4(SbPh_3)_2$; all were close to 1/3, which confirms the axial nature of the resonant transition.[9,14] These results indicate that, although the principal geometric change on excitation is along the Rh–Rh coordinate, there are small consequential geometric changes along many other coordinates—changes associated not only with the acetate rings but also, and more surprisingly, with X-sensitive modes of the phenyl rings. It is hoped, in future analyses, to be able to quantify these changes.

The principal progression-forming mode (ν_1) in each resonance Raman spectrum is almost harmonic; thus, for the $AsPh_3$ complex, $\omega_1 = 297.2$ cm^{-1} and $x_{11} = -0.16$ cm^{-1} while, for the $SbPh_3$ complex, $\omega_1 = 307$ cm^{-1} and $x_{11} = 0.0$ cm^{-1}. This mirrors the similar behavior displayed by the analogous PPh_3 complex.[8]

Acknowledgment. We thank the SERC and the ULIRS for financial support.

Registry No. $Rh_2(O_2CCH_3)_4(AsPh_3)_2$, 34767-18-5; $Rh_2(O_2CCH_3)_4(SbPh_3)_2$, 100237-77-2.

Supplementary Material Available: Tables VIII and IX, containing full band listings and assignments for the infrared spectra of the $AsPh_3$ and $SbPh_3$ complexes (4 pages). Ordering information is given on any current masthead page.

(14) Mortensen, O. S.; Hassing, S. In *Advances in Infrared and Raman Spectroscopy*; Clark, R. J. H., Hester, R. E., Eds.; Heyden: London, 1980; Vol. 6, pp 1-60.

Contribution from the Departments of Chemistry, NREC College, Khurja-203131 (UP), India, and Indian Institute of Technology, Hauz Khas, New Delhi-110016, India

Magnetic and Spectroscopic Characterization of the High-Spin ($^6A_1$) ⇌ Low-Spin ($^2T_2$) Transition in an Iron(III) Complex of Pyridoxal Thiosemicarbazone

Madan Mohan,*[,†] Puranam H. Madhuranath,[†] Alok Kumar,[†] Munesh Kumar,[†] and Narendra K. Jha[‡]

Received April 8, 1988

The preparation and characterization of the new discontinuous ferric spin-crossover complex $[Fe(HL)_2]Cl$ and the hydrated low-spin form of the complex $[Fe(HL)_2]Cl\cdot 2H_2O$ are reported. In these complexes HL^- is the deprotonated form of pyridoxal thiosemicarbazone (H_2L) acting as an ONS tridentate ligand. The magnetic moments for the spin-crossover complex show a thermal hysteresis, where with sample cooling the transition temperature is 245 K and with sample heating it is 256 K. Variable-temperature ^{57}Fe Mössbauer and EPR data also provide evidence for the presence of a first-order phase transition in this complex. It is most likely that the cooperative (first-order) nature of this transition is due to the extended coupling of ferric complexes through intermolecular hydrogen-bonding interactions. EPR spectra of the two complexes in this study show that both have a singly occupied d_{xy} orbital in the ground Kramers doublet.

Introduction

Thermally driven transitions between high-spin and low-spin ground states in iron compounds have recently been the subject of numerous investigations.[1-4] It has been demonstrated that transitions of the type high spin ⇌ low spin may exhibit either an essentially discontinuous or a more gradual behavior.[4-6] The discontinuous spin-crossover transformations have been shown, on the basis of heat capacity measurements,[7-9] to be thermodynamically first-order.[10] Moreover, the observation of hysteresis[4] has been employed as an indication of the first-order character of the abrupt spin transformations. Recently, variable-temperature X-ray diffraction measurements have also revealed that discon-

[†] NREC College.
[‡] Indian Institute of Technology.

(1) König, E.; Ritter, G.; Irler, W.; Goodwin, H. A. *J. Am. Chem. Soc.* **1980**, *102*, 4681.
(2) König, E.; Ritter, G.; Kulshreshtha, S. K.; Nelson, S. M. *J. Am. Chem. Soc.* **1983**, *105*, 1924.
(3) Purcell, K. F.; Edwards, M. P. *Inorg. Chem.* **1981**, *23*, 2620.
(4) Gütlich, P. *Struct. Bonding (Berlin)* **1981**, *44*, 83.
(5) Goodwin, H. A. *Coord. Chem. Rev.* **1976**, *18*, 293.
(6) Martin, R. L.; White, A. H. *Transition Met. Chem. (Weinheim, Ger.)* **1968**, *4*, 113.
(7) Sorai, M.; Seki, S. *J. Phys. Soc. Jpn.* **1972**, *33*, 575.
(8) Sorai, M.; Seki, S. *J. Phys. Chem. Solids* **1974**, *35*, 555.
(9) Shipilov, V. I.; Zelentsov, V. V.; Zhadanov, V. M.; Turdakin, V. A. *JETP Lett. (Engl. Transl.)* **1974**, *19*, 294.

0020-1669/89/1328-0096$01.50/0

tinuous lattice modifications (and concomitant unit cell volume changes) accompany these spin transitions.[1,11-13] These findings are in keeping with the first-order nature of such transitions. Although relatively little is known about the microscopic origin of such transitions, it seems that discontinuous spin transitions arise for compounds with strong cooperative (i.e., intermolecular) interactions.

The ferric thiosemicarbazones, particularly those formed with pyruvic acid thiosemicarbazone (I) and salicylaldehyde thiosemicarbazone (II),[14-24] are of considerable interest owing to their discontinuous spin transitions among the various six-coordinate ferric spin-crossover compounds. The spin-crossover properties

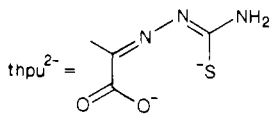

Y[Fe(thpu)2]•nH2O (I)

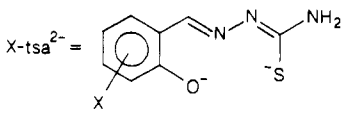

Y[Fe(X-tsa)2]•nH2O (II)

for these compounds are quite sensitive to changes in the outer-sphere cation Y, the number of water molecules, and the nature of the substituent X attached to the salicylaldehyde moiety. Recently, the magnetic, spectroscopic, and structural characterization of the discontinuous ferric spin-crossover complex [Fe(Hthpu)(thpu)], where $Hthpu^-$ and $thpu^{2-}$ are deprotonated forms of pyruvic acid thiosemicarbazone, have been reported.[25]

In the present paper, we report variable-temperature magnetic and spectroscopic characterization of the discontinuous spin crossover in a new ferric thiosemicarbazone complex, $[Fe(HL)_2]Cl$, where HL^- is the anion of pyridoxal thiosemicarbazone. In addition, the characterization of the hydrated form $[Fe(HL)_2]Cl\cdot 2H_2O$ is also reported.

Experimental Section

Compound Preparation. Commercially available starting materials were used without further purification. Elemental C, H, and N analyses were carried out on a Perkin-Elmer Model 240C automatic instrument.

Pyridoxal Thiosemicarbazone. A solution of pyridoxal hydrochloride (0.21 g), in its neutral form, in 30 mL of ethanol was added with constant stirring to thiosemicarbazide (0.091 g) in 30 mL of ethanol, and the solution mixture was refluxed for 30 min. After the mixture was cooled, a deep yellow microcrystalline product was isolated by filtration, washed with alcohol, and dried in vacuo. Anal. Calcd for $C_9H_{12}N_4SO_2$: C, 45.00; H, 5.00; N, 23.33. Found: C, 44.92; H, 4.95; N, 23.17. The compound has a melting point of 228 °C and is soluble in water and warm ethanol and scarcely in chloroform.

$[Fe(HL)_2]Cl$. A hot solution of pyridoxal thiosemicarbazone (0.24 g, 10 mmol) in 30 mL of ethanol was added dropwise with constant stirring to a solution of anhydrous $FeCl_3$ (0.81 g, 5 mmol) in 25 mL of ethanol. The resulting solution mixture was heated under reflux for 30 min and then kept overnight at room temperature. The dark brown microcrystals were isolated by filtration, washed with ethanol and diethyl ether, and dried in vacuo over P_2O_5; mp 240 °C. Anal. Calcd for $FeC_{18}H_{22}N_8S_2O_4Cl$: C, 37.94; H, 3.86; N, 19.67; Fe, 9.80. Found: C, 37.82; H, 3.80; N, 19.54; Fe, 9.88.

$[Fe(HL)_2]Cl\cdot 2H_2O$. A solution of $FeCl_3$ (0.81 g, 5 mmol) in 20 mL of water was added dropwise with stirring to a solution of pyridoxal thiosemicarbazone (0.24 g, 10 mmol) in 15 mL of water. The resulting solution was heated under reflux for about 30 min and allowed to stand at room temperature to give dark brown microcrystals. The microcrystals were isolated by filtration, washed with water, and dried. Anal. Calcd for $FeC_{18}H_{26}N_8S_2O_6Cl$: C, 35.68; H, 4.29; N, 18.50; Fe, 9.21. Found: C, 35.57; H, 4.21; N, 18.42; Fe, 9.27.

Physical Measurements. Variable-temperature magnetic susceptibility data were obtained on a vibrating-sample magnetometer, operated at 5 kG. The magnetometer was calibrated with $CuSO_4\cdot 5H_2O$, and a calibrated GaAs diode was used for sample temperature determination and control. For all data, diamagnetic corrections, estimated from Pascal's constants,[26] were used in the calculation of molar paramagnetic susceptibilities.

Electron paramagnetic resonance data (X-band) were obtained on a Varian E-4 spectrometer, using DPPH as a reference material. Variable temperatures (300–77 K) were obtained with the use of a gas-flow cavity insert in conjunction with a Varian V-4540 temperature controller. Temperatures were determined before and after each spectrum with a copper–constantan thermocouple, and the temperature accuracy was estimated to be ±5 K. A direct-immersion Dewar, which was inserted into the cavity, was used to obtain spectral data at 77 K.

^{57}Fe Mössbauer spectral data were collected on polycrystalline samples by using a constant-acceleration spectrometer that was calibrated with natural α-iron foil. The source was $^{57}Co(Cu)$ and was maintained at room temperature for all experiments. A copper–constantan thermocouple, mounted on the sample cell holder, was used to monitor the sample temperature. The absolute precision is estimated to be ±3 K. A computer program was used to fit the Mössbauer absorptions to Lorentzian line shapes. The isomer shifts are reported with respect to natural iron foil at 298 K.

The molar conductances for the samples in methanol (1×10^{-3} mol/L) at 25 °C were measured on a Toshniwal conductivity bridge, Type CL 01/01.

Results and Discussion

The infrared spectrum of the free ligand pyridoxal thiosemicarbazone (H_2L) exhibits absorption bands at 3140 m and 2860 sh cm^{-1}, which are assigned to $\nu(NH)$ and $\nu(NH^+)$ of the pyridine ring whose protonation has occurred due to migration of the phenolic OH group to the pyridine nitrogen,[27,28] respectively. No bands are observed at ca. 2500 cm^{-1} assignable to the SH group. Thus, the free ligand (H_2L) exists in the thione form (III) in the

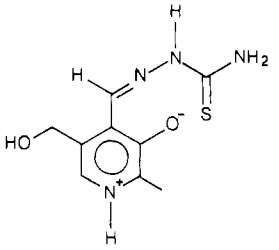

III

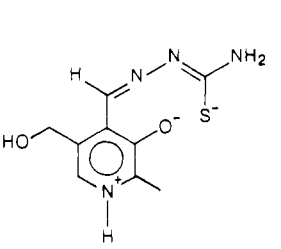

IIIa

solid state. However, in solution and in the presence of some metal ions the ligand may exist in equilibrium with the tautomeric form IIIa. The tautomer IIIa formed by the loss of the thiol proton might be expected to act as a charged tridentate ligand by coordinating to a metal ion through the mercapto sulfur, the azomethine nitrogen, and the phenolic oxygen.

(10) Kittel, C.; Kroemer, H. *Thermal Physics*; W. H. Freeman: San Francisco, CA, 1980; Chapter 10.
(11) Irler, W.; Ritter, G.; König, E.; Goodwin, H. A.; Nelson, S. M. *Solid State Commun.* **1979**, *29*, 39.
(12) König, E.; Ritter, G.; Kulshreshtha, S. K.; Waigel, J.; Goodwin, H. A. *Inorg. Chem.* **1984**, *23*, 1896.
(13) König, E.; Ritter, G.; Kulshreshtha, S. K. *Chem. Rev.* **1985**, *85*, 219.
(14) Ivanov, E. V.; Zelentsov, V. V.; Gerbeleu, N. V.; Ablov, A. V. *Dokl. Chem. (Engl. Transl.)* **1970**, *191*, 249.
(15) Zelentsov, V. V.; Ablov, A. V.; Turta, K. I.; Stukan, R. A.; Gerbeleu, N. V.; Ivanov, E. V.; Bogdanov, A. P.; Barba, N. A.; Bodyu, V. G. *Russ. J. Inorg. Chem. (Engl. Transl.)* **1972**, *17*, 1000.
(16) Zelentsov, V. V.; Bogdanova, L. G.; Ablov, A. V.; Gerbeleu, N. V.; Dyatlova, Ch. V. *Dokl. Chem. (Engl. Transl.)* **1972**, *207*, 864.
(17) Zelentsov, V. V.; Larin, G. M.; Ivanov, E. V.; Gerbeleu, N. V.; Ablov, A. V. *Theor. Exp. Chem. (Engl. Transl.)* **1971**, *7*, 648.
(18) Ablov, A. V.; Zelentsov, V. V.; Shipilov, V. I.; Gerbeleu, N. V.; Dyatlova, Ch. V. *Dokl. Phys. Chem. (Engl. Transl.)* **1975**, *222*, 567.
(19) Turta, K. I.; Ablov, A. V.; Gerbeleu, N. V.; Dyatlova, Ch. V.; Stukan, R. A. *Russ. J. Inorg. Chem. (Engl. Transl.)* **1976**, *21*, 266.
(20) Ablov, A. V.; Goldanskii, V. I.; Turta, K. I.; Stukan, R. A.; Zelentsov, V. V.; Ivanov, E. V.; Gerbeleu, N. V. *Dokl. Phys. Chem. (Engl. Transl.)* **1971**, *196*, 134.
(21) Ryabova, N. A.; Ponomarev, V. I.; Atovmyan, L. O.; Zelentsov, V. V.; Shipilov, V. I. *Sov. J. Coord. Chem. (Engl. Transl.)* **1978**, *4*, 95.
(22) Ryabova, N. A.; Ponomarev, V. I.; Zelentsov, V. V.; Atovmyan, L. O. *Sov. Phys.—Crystallogr. (Engl. Transl.)* **1981**, *26*, 53.
(23) Ryabova, N. A.; Ponomarev, V. I.; Zelentsov, V. V.; Atovmyan, L. O. *Sov. Phys.—Crystallogr. (Engl. Transl.)* **1982**, *27*, 46.
(24) Ryabova, N. A.; Ponomarev, V. I.; Zelentsov, V. V.; Atovmyan, L. O. *Sov. Phys.—Crystallogr. (Engl. Transl.)* **1982**, *27*, 171.
(25) Timken, M. D.; Wilson, S. R.; Hendrickson, D. N. *Inorg. Chem.* **1985**, *24*, 3450.
(26) Figgis, B. N.; Lewis, J. In *Modern Coordination Chemistry*; Lewis, J., Wilkinson, R. G., Eds.; Interscience: New York, 1960; p 403.
(27) Domiano, P.; Musatti, A.; Nardelli, M.; Pelizzi, C.; Predieri, G. *Transition Met. Chem.* **1979**, *4*, 351.
(28) Matsushima, Y. *Chem. Pharm. Bull.* **1968**, *16*, 2143.

Table I. Selected Vibrational Bands (cm^{-1}) of Pyridoxal Thiosemicarbazone and Its Iron(III) Complexes

compd	$\nu(NH_2)$, $\nu(OH)$	$\nu(NH)$	$\nu(NH^+)$	$\nu(C{=}N)$, $\nu(C{=}C)$	ring	$\nu(C{=}N)$	ring	$\nu(OH)$	$\nu(C{=}O)$	$\nu(N{-}N)$	$\nu(C{=}S)$
H_2L	3430 m 3280 m	3140 m	2860 sh	1600 s	1575 s	1530 s	1495 m 1465 m 1430 s 1415 sh	1375 vs	1290 m	1060 m	935 m
$[Fe(HL)_2]Cl$	3440 mb 3240 m		2880 w	1630 s 1610 s	1590 s	1560 m	1495 s 1470 m 1420 w 1410 w	1375 vs	1300 m	1030 m	850 m
$[Fe(HL)_2]Cl{\cdot}2H_2O$	3440 mb 3240 m		2875 w	1620 m 1610 s	1590 s	1560 m	1495 m 1460 m 1425 m 1415 sh	1375 s	1300 m	1035 m	860 m

When the solution of the free ligand in ethanol or water IIIa was heated under reflux with an ethanolic or aqueous solution of $FeCl_3$, it afforded a dark brown microcrystalline complex of the formula $[Fe(HL)_2]Cl$ or $[Fe(HL)_2]Cl{\cdot}2H_2O$, respectively. The complexes are quite stable at room temperature and do not show any decomposition after a long period of standing. The complexes are soluble in a number of solvents of moderate-to-good coordinating ability, such as dimethylformamide, dimethyl sulfoxide, methanol, ethanol, and pyridine. The molar conductances of 10^{-3} M $[Fe(HL)_2]Cl$ and $[Fe(HL)_2]Cl{\cdot}2H_2O$ in methanol at 25 °C are 110 and 118 Ω^{-1} cm^2 mol^{-1}, indicating[29] their uni-univalent electrolytic behavior in solution. The complexes exhibit sharp melting points.

Infrared Spectra. The main vibrational bands of the free ligand (H_2L) and its ferric complexes are reported in Table I. In the NH stretching frequency region, the spectral band ν(NH) disappears in the complexes, indicating the deprotonation of the NH group.[30] The coordination of the azomethine nitrogen atom to the ferric ion is indicated by the shifting of the bands chiefly assigned to ν(N—N) and ν(C=N) stretching vibrations.[31] The slight shift of ν(C—O(phenolic)) in the complex may be ascribed[32] to a delocalization of electron density from the oxygen atom to the metal ion, resulting in a slight ionic character of the C–O bond and consequently a slight shift in the ν(C—O) frequency. The low-frequency shift of ν(C=S) stretching from 935 s cm^{-1} in the free ligand to approximately 860 cm^{-1} in ferric complexes is indicative of involvement of the sulfur atom in bonding to the metal. In the far-infrared spectra, the ferric complexes exhibit bands at about 425, 370, and 330 cm^{-1}, which are assigned to Fe—O(phenolic), Fe—S, and Fe—N stretching vibrations, respectively.

Magnetic Susceptibility. The variable-temperature magnetic susceptibility data for $[Fe(HL)_2]Cl$ between 78 and 300 K are presented in Figure 1. From Figure 1 it may be easily visualized that the effective magnetic moment decreases smoothly from μ_{eff} = 5.75 μ_B at 299 K to μ_{eff} = 4.00 μ_B at 245 K, whereupon a sharp drop to μ_{eff} = 2.26 μ_B at 230 K is observed. To lower temperatures an almost temperature-independent range of μ_{eff} values follows down to μ_{eff} = 2.01 μ_B at 78 K. Thus, on the basis of magnetism, the transition temperature associated with the $^6A_1 \rightleftharpoons {}^2T_2$ spin transition is well defined as $T_c(\downarrow)$ = 245 K. For the reverse transition that occurs upon sample heating, $T_c(\uparrow)$ is 256 K. A thermal hysteresis of 11 K is present. The abruptness of the transition and the observation of thermal hysteresis lead us to conclude that the discontinuous nature of the thermal spin-crossover transformation for $[Fe(HL)_2]Cl$ is a first-order phase transition. The hydrated complex exhibits a magnetic moment of 2.05 μ_B at room temperature (299 K), suggesting that it is predominantly in the low-spin state.

Mössbauer Spectroscopy. Variable-temperature ^{57}Fe Mössbauer spectra of $[Fe(HL)_2]Cl$ are illustrated in Figure 2. At 298 K,

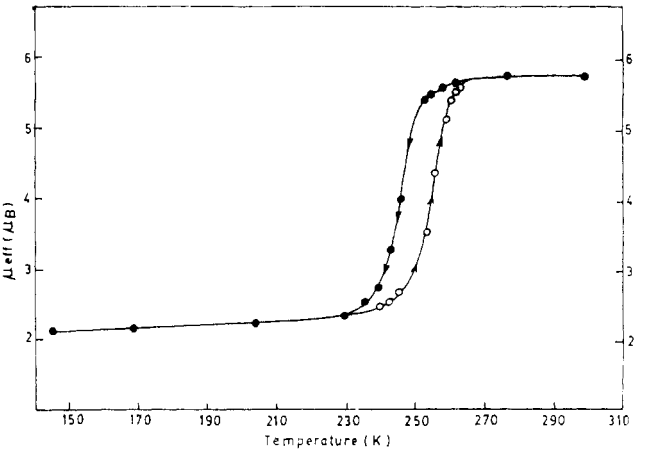

Figure 1. Effective magnetic moments of $[Fe(HL)_2]Cl$ as a function of temperature: (●) cooling; (○) heating. The solid lines are drawn for purposes of clarity only and do not represent data fittings or simulations.

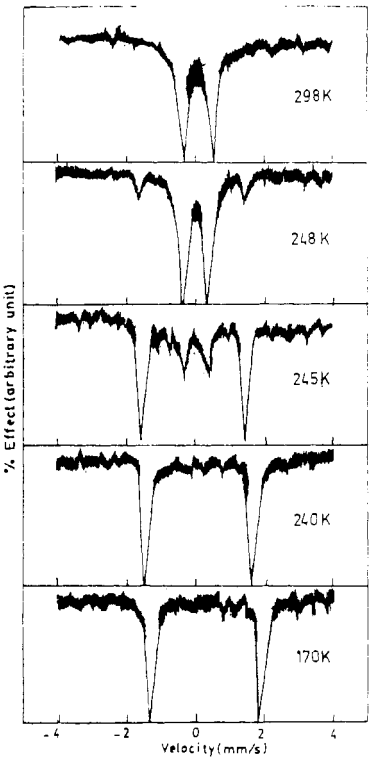

Figure 2. Mössbauer spectra for $[Fe(HL)_2]Cl$ at selected temperatures.

the ^{57}Fe Mössbauer spectrum consists of a single doublet characterized by the quadrupole splitting ΔE_Q = 0.84 mm/s and isomer shift δ = 0.48 mm/s. On the basis of the values of ΔE_Q and δ, it is justified to assign this spectrum to high-spin iron(III) in approximately pseudooctahedral ($^6A_1$) coordination. Additional support for the assignment is provided by the magnetic data; e.g.,

(29) Geary, W. J. *Coord. Chem. Rev.* **1971**, *7*, 81.
(30) Iskander, M. F.; El-Sayed, L. *J. Inorg. Nucl. Chem.* **1971**, *33*, 4253.
(31) Mohan, M.; Sharma, P.; Kumar, M.; Jha, N. K. *Inorg. Chim. Acta* **1986**, *125*, 9.
(32) Mohan, M.; Tandon, J. P.; Gupta, N. S. *Inorg. Chim. Acta* **1986**, *111*, 187.

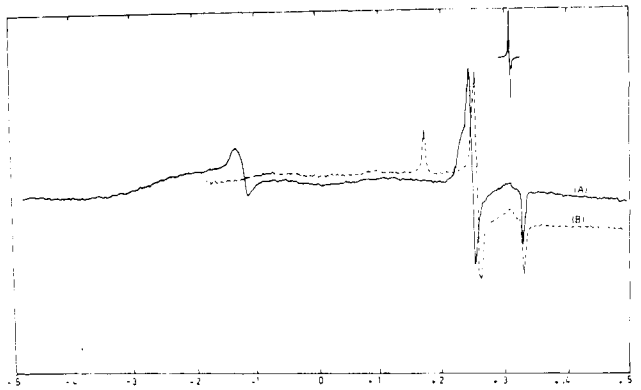

Figure 3. X-Band EPR spectra at 77 K for $[Fe(HL)_2]Cl$ (A) and $[Fe(HL)_2]Cl\cdot 2H_2O$ (B).

μ_{eff} = 5.75 μ_B at 299 K (Figure 1). At 275 K, a slight asymmetry of the spectrum appears, becomes more pronounced at 260 K, and increases further with decreasing temperature. The origin of the asymmetry is a second doublet, which may be clearly distinguished only at 248 K. The intensity of this doublet, expressed by the (uncorrected) fractional area, amounts at 248 K to about 20%. On the basis of the quadrupole splitting ΔE_Q = 3.08 mm/s and the isomer shift δ = 0.20 mm/s (both at 248 K), the new doublet may be assigned to the $^2T_2$ ground state of low-spin iron(III). The assignment is consistent with the decrease of the magnetic moment to μ_{eff} = 2.74 μ_B at 240 K. As the sample temperature is lowered further, the intensity of the high-spin doublet decreases dramatically between 248 and 245 K and goes to zero below 240 K, while that of the outer low-spin quadrupole-split doublet increases at the same rate in the same temperature range. As expected, there is a change of the ground-state effective magnetic moment from μ_{eff} = 5.75 μ_B at 299 K to μ_{eff} = 2.26 μ_B at 230 K (Figure 1). The present results clearly demonstrate that in $[Fe(HL)_2]Cl$ the high-spin ($^6A_1$) $\rightleftharpoons$ low-spin ($^2T_2$) transition takes place over the temperature range 150–298 K, the transition being centered at about 245 K.

At 150 K, the ^{57}Fe Mössbauer spectra of $[Fe(HL)_2]Cl$ and $[Fe(HL)_2Cl\cdot 2H_2O$ are quite similar. For the nonhydrated compound, the quadrupole splitting ΔE_Q is 3.11 mm/s and the isomer shift δ is 0.20 mm/s. For the hydrated material, ΔE_Q = 3.12 mm/s and δ = 0.18 mm/s. All of these parameters are characteristic for low-spin ferric centers.

Electron Paramagnetic Resonance. Figure 3 illustrates the X-band EPR spectra at 77 K of both low-spin materials. It is clear that the spectra of hydrated and nonhydrated solids are quite different. The EPR signal of the hydrated ferric material is characterized by rhombic symmetry in contrast with axial symmetry in the nonhydrated ferric solid. The experimental anisotropic g values for the low-spin state of these solids, listed in Table II, were analyzed[33] to determine the nature of the ground-state Kramers doublet. It can be concluded that the unpaired electron in the ground Kramers doublet is in a d_{xy} orbital. This result is in agreement with Mössbauer spectral data (vide supra). Furthermore, the g-value analysis indicates that the first excited Kramers doublet is much higher in energy than the ground-state Kramers doublet (assuming spin–orbit coupling (Fe^{III}) of 460 cm^{-1}). This energy separation, much larger than the thermal energies, indicates that the low-spin magnetic moment and Mössbauer quadrupole splitting should be essentially temperature-independent.

A very broad signal (full width at half-height ~2 kG) centered at ~1.2 kG (g_{eff} = 3.13) was observed in the X-band EPR spectrum of the nonhydrated ferric sample at room temperature. However, a weak signal at g = 4.3 was observed for this sample at 77 K (Figure 3). High-spin EPR signals for molecular solids of this type typically are found in the low-field region (1–2.5 kG at X-band frequencies) because the zero-filled splitting in the high-spin state is gauged by $\hat{H} = D\hat{S}_{z^2} + E(S_x^2 - S_y^2)$, where D and E are the axial and rhombic zero-field splitting parameters, respectively.[34] The presence of a strong signal g = ca. 4.3 indicates that the molecular symmetry is low (rhombic) and $E/D \simeq 1/3$ and $h\nu/D \leq 3$, where $h\nu$ is the microwave energy (ca. 0.3 cm^{-1} at X-band frequencies). At low temperature, the signal at g = ca. 2 is well resolved and is characterized by axial symmetry in contrast with rhombic symmetry in the high-spin state. The difference of the molecular symmetry between the low- and high-spin states plays an important role in the spin-exchange mechanism. However, we attribute the extremely broad line width to short relaxation times of spin–spin mechanisms enhanced by short dipole–dipole (i.e., Fe–Fe) interactions.

Table II. Experimental and Calculated[a] EPR Parameters

	$[Fe(HL)_2]Cl$	$[Fe(HL)_2]Cl\cdot 2H_2O$		$[Fe(HL)_2]Cl$	$[Fe(HL)_2]Cl\cdot 2H_2O$
g_x	2.245	2.390	A_2	0.991	0.810
g_y	2.245	2.131	B_2	0.098	−0.113
g_z	1.920	1.921	C_2	0	−0.645
δ/ξ	2.35	2.52	E_2/ξ	2.001	0.550
ϵ/ξ	0	−1.03	A_3	0.995	0.650
A_1	0.107	0.114	B_3	0.096	−0.046
B_1	0.993	0.993	C_3	0	−0.758
C_1	0	−0.044	E_3/ξ	3.197	5.712
E_1/ξ	−4.701	−5.210			

[a] Parameter definitions and methods of calculations are described in the text.

Conclusion

A number of recent research efforts in the area of spin-crossover chemistry have centered on better characterization of the factors that influence the bulk properties of the solid-state transformation.[4,35] It has been suggested[1,2] repeatedly that discontinuous transformations are essentially first-order phase transitions, where high- and low-spin domains are present and cooperative intermolecular interactions play an important role. An important factor that may be responsible for discontinuous spin-crossover transitions in ferric thiosemicarbazones is the abundance of potential sites for intermolecular hydrogen-bonding interactions responsible for strong coupling of the monomeric units in the solid state.[25,36,37] Thus, the cooperative nature of the spin-crossover transformation in $[Fe(HL)_2]Cl$ may be due to extended coupling of ferric complexes through intermolecular hydrogen bonds. Such hydrogen-bonding interactions have been noted[38,39] in other structurally characterized discontinuous spin-crossover solids.

Acknowledgment. We are grateful to Professors David H. Petering and William Antholine, Department of Chemistry, University of Wisconsin—Milwaukee, Milwaukee, WI 53201, for carrying out EPR studies under an ICRETT award, UICC, Switzerland. The support of this work by the Department of Science and Technology, New Delhi, India, is also gratefully acknowledged.

(33) Bohan, T. L. *J. Magn. Reson.* **1977**, *26*, 109.
(34) Wickman, H. H.; Klein, M. P.; Shirley, D. A. *J. Chem. Phys.* **1965**, *42*, 2115.
(35) Zimmermann, R. *J. Phys. Chem. Solids* **1983**, *44*, 151.
(36) Mathew, M.; Palenik, G. J. *J. Am. Chem. Soc.* **1969**, *91*, 6310.
(37) Mathew, M.; Palenik, G. J. *Inorg. Chim. Acta* **1971**, *5*, 349.
(38) Katz, B. A.; Strouse, C. E. *J. Am. Chem. Soc.* **1979**, *101*, 6214.
(39) Mikami, M.; Konno, M.; Saito, Y. *Chem. Phys. Lett.* **1979**, *63*, 566.